

Interference Effects on a Multi-GNSS Receiver On-Board a CubeSat in LEO

Austin McKibben, Ryan McKnight, Brian C. Peters, Zachary Arnett, Sabrina Ugazio, *Ohio University*

BIOGRAPHY

Austin McKibben is pursuing his Master's in Electrical Engineering at Ohio University as a part of the Avionics Engineering Center. His research interests include global navigation satellite systems (GNSS) interference and signal monitoring. He received his B.S. in Computer Science from Ohio University in 2022.

Ryan McKnight is pursuing his Ph.D. in Electrical Engineering and Computer Science at Ohio University as part of the Avionics Engineering Center. His research interests include GNSS inter-constellation time offset determination and radio-frequency pulsar navigation and timing. He was previously involved with development and operations of the Bobcat-1 CubeSat. He received his B.S. in Electrical Engineering from Ohio University in 2019.

Brian C. Peters is pursuing his Ph.D. in Electrical Engineering and Computer Science at Ohio University as part of the Avionics Engineering Center. He completed his M.S. in Electrical Engineering at Ohio University in 2021 where he was involved in the development and operation of the Bobcat-1 CubeSat and conducted research on estimation of GNSS inter-constellation time offsets. He was also involved in the development of the Cislunar Autonomous Positioning System demonstration for NASA's CAPSTONE mission.

Zachary Arnett is pursuing his Ph.D. in Electrical Engineering and Computer Science at Ohio University as part of the Avionics Engineering Center. His research interests include GNSS inter-constellation time offset determination and radio-frequency pulsar navigation and timing. He received his B.S. in Electrical Engineering from Ohio University in 2019.

Sabrina Ugazio is an Assistant Professor in Electrical Engineering and Computer Science at Ohio University. She received her Ph.D. in Electronics and Telecommunications Engineering from Politecnico di Torino in 2013. Her current research interests include PNT for space applications, autonomous systems, timing, remote sensing.

ABSTRACT

Given the increasing number of critical applications relying on GNSS, GNSS spectrum monitoring is becoming more and more crucial. Monitoring from Low Earth Orbit (LEO) has been investigated, and interference-source geolocation demonstrated. In this paper results are shown from the Bobcat-1 CubeSat mission, which enables multi-GNSS measurements but was not optimized for spectrum monitoring. The analysis of the power metrics suggests that non ad-hoc GNSS measurements from LEO could be exploited for GNSS spectrum monitoring scope.

I. INTRODUCTION

The monitoring of global navigation satellite systems (GNSS) interference is a topic of global interest and widespread research, as Allen (2023) highlights, including "GPS monitoring, disruption, public warning, and risk assessment" among the recommendations. GNSS interference can manifest in various forms, both intentional and unintentional (Ward et al., 2017). Several methods have been proposed and used to identify, characterize, and localize sources of harmful interference. The use of historical automatic dependent surveillance-broadcast (ADS-B) data has been proposed to localize interference sources in real-time (Dacus et al., 2022; Liu et al., 2022; Nasser et al., 2022). Jada et al. (2022) analyzes GNSS data collected on U.S. highways to identify and predict interference events. Monitoring through android devices has also been proposed (Spens et al., 2022).

Several previous works have analyzed the effects of various forms of intentional and unintentional L-band jamming on commercial GNSS receivers in terrestrial applications, and detailed studies have been presented that provide theoretical analysis and models (Borio et al., 2012; Falletti et al., 2021; Nasser et al., 2022). In addition to various terrestrial monitoring methods, robust monitoring of GNSS interference from low Earth orbit (LEO) has been demonstrated and shown to be viable (CaJacob et al., 2016; Clements et al., 2022, 2023; Ellis et al., 2022; *GNSS Interference Report: Finland*, 2022; LaChapelle et al., 2021; Murrian et al., 2021). Strong sources of interference can also impact GNSS users in LEO and result in temporary loss of positioning, navigation, and timing (PNT) services as spacecraft pass overhead. Though the duration of these effects are typically relatively short due to the high relative speed of LEO satellites, terrestrial interference can still be observed to significantly impact receivers in space. In Clements et al. (2022), geolocation of terrestrial spoofing sources with accuracy within 10 km has been validated,

with a LEO single-satellite and a single-pass. In Clements et al. (2023), time difference of arrival (TDOA) and frequency difference of arrival (FDOA) are exploited to geolocalize terrestrial jamming emitters with two LEO. Real-time characterization and localization of interference sources can be used to inform terrestrial users and avoid areas where poor GNSS performance is expected. While ad-hoc systems for interference detection in general include features to enable accurate geolocalization of the emitters, monitoring capabilities of non-ad hoc and even low-cost devices are more and more of interests. For example, recent research presented in Miguel et al. (2022) extensive testing is conducted to analyze power metrics (power spectral density (PSD), automatic gain control (AGC) and carrier-to-noise ratio (C/N_0)) in a low cost commercial receiver, in various controlled scenarios including either spoofing or different types of jamming. In Miguel et al. (2023) the power metrics are analyzed in different interference scenarios and for different receivers, for calibration purposes, with the goal of setting opportune thresholds on the power metrics, to enable interference detection. It shall be noted that a power metric often used to characterize the presence of interference is the carrier-to-noise ratio, C/N_0 . Also in this paper the C/N_0 estimate will be considered. However, it is important to keep in mind that in the presence of interference, what is usually identified as C/N_0 is actually an estimate of the carrier-to-interference-and-noise ratio, referred to as carrier-to-interference-and-noise ratio (CIN_0), as the theoretical background provided in Teunissen and Montenbruck (2017) clarifies.

In this paper, power metrics collected by the Bobcat-1 CubeSat are shown. The CubeSat, developed at Ohio University's Avionics Engineering Center, collected GNSS data using a NovAtel OEM719 (*OEM7 Commands and Logs Reference Manual*, 2023) in LEO from November 2020 until April 2021. Bobcat-1's primary mission was not related to interference detection, indeed the goal was to support the estimation of system-to-system time offsets using multi-frequency and multi-constellation measurements across all operational systems and signals (Arnett et al., 2022). In addition to these data collections dedicated to time offset estimation, Bobcat-1 performed a number of collections including PSD measurements, aimed at observing and analyzing the GNSS signal spectrum using NovAtel's Interference Toolkit (ITK). Several interference events were recorded by Bobcat-1 across all data collection types throughout its lifetime.

The OEM719 receiver aboard Bobcat-1 was configured to track all currently available signals from Global Positioning System (GPS), Globalnaya Navigazionnaya Sputnikovaya Sistema, or Global Navigation Satellite System (GLONASS), Galileo, BeiDou, QZSS, and NavIC. An Antcom G5ANT-1.9AS-1-3 patch antenna (with 33 dB internal low-noise amplifier (LNA)) was mounted to Bobcat-1's +Z face. The patch antenna was routed to the OEM719 through a 10 dB attenuator to preserve the dynamic range of the receiver. A cutaway view of Bobcat-1 is given in Figure 1 which displays the hardware configuration. Bobcat-1 had no active attitude control, and only possessed the capability to detumble using several magnetorquers. For most data collections, Bobcat-1 was configured to remain in detumbling mode which reduced the CubeSat's rotation using a B-Dot detumbling algorithm. Fewer collections were performed with detumbling off.

The data collections performed by Bobcat-1 using the OEM719 contained, at a minimum, C/N_0 measurements for all tracked satellites, the OEM719's current position estimate, and data from the receiver's onboard temperature sensors. Spectrum data additionally contain ITPSDFINAL and less frequently SPRINKLERDATA messages, which provide PSD data and in-phase/quadrature (I/Q) samples (respectively) in the L1 band. Bobcat-1's spectrum data collections were configurable, however, and not all contain the same messages. Experimentation with these collections continued throughout the mission, with some attempting to automatically determine the presence of interference through computation of a jamming-to-signal ratio using PSD samples before enabling raw I/Q collection. This was done primarily in the interest of reducing the total amount of data produced due to downlink limitations. Despite the primary mission of Bobcat-1 was not focused on spectrum monitoring, interesting results can be retrieved observing the available power metrics. As results available in the literature suggest, as for instance (Miguel et al., 2022, 2023), the power metrics seem to be valid measurement for interference detection. To further validate the result, comparison between different power metrics have been done, comparing the AGC and the C/N_0 metrics against the PSD. PSD measurements provide a more direct observations of the interference effects, but given the scope of the mission PSD measurements have been collected only during specific test data collections. C/N_0 estimates are available during all data collections, but it shall be noticed that drops in C/N_0 could be due to several causes, including changes in the spacecraft's attitude. Comparisons between the metrics are done, to correlate the C/N_0 drops and the actual presence of interference, with the objective to extend the analysis to the collections where PSD were not available. Only a limited number of data collections are shown in this paper, but more data have been analyzed; the data considered so far show consistency between C/N_0 (or AGC) anomalies and interference detected on the PSD, suggesting that those metrics could provide useful observables of interference events. Small satellites in LEO provided with low cost GNSS receivers for other scopes may provide relevant measurements for GNSS spectrum monitoring scopes, and even emitter detection. The results shown in this paper indicate that the power metrics can provide a loose geolocalization solution. Further analysis will aim to calibrate the effect of the receiving antenna including attitude estimate, as well as quantitatively estimating the interference-to-signal ratio.

II. ANALYSIS

The data collected from Bobcat-1's on-board NovAtel OEM7 GNSS receiver comprises several distinct "collections", each with a unique collection ID number (numbered sequentially starting with the first on-orbit data collection). Several distinct types

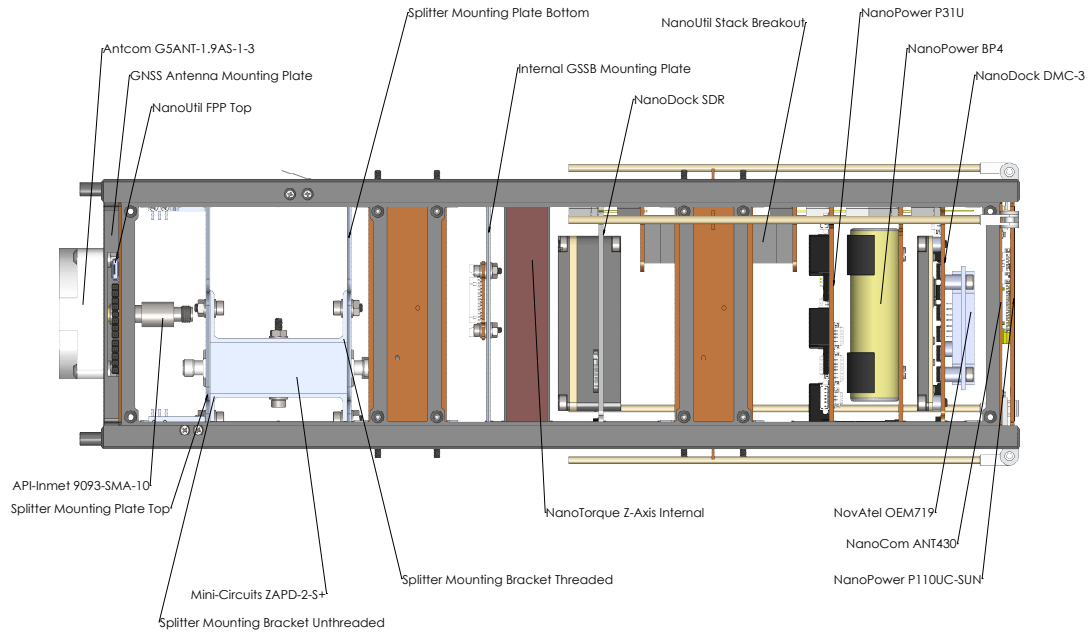


Figure 1: Bobcat-1 cutaway view

of data collections were performed in order to support Bobcat-1’s various primary and secondary mission goals. These types included “Time Offset” collections, “Spectrum” collections, and “Antenna Patterns” collections, among others. Each distinct collection type was configured with its own settings for the type, format, and rate of measurements that were collected from the on-board OEM7 receiver. During the in-orbit lifetime of Bobcat-1, over 250 data collections were performed in total. The results presented in this paper are taken from the data contained within 3 individual collections with ID numbers 13, 178, and 181. These particular collections were selected due to analysis which revealed strong indications of interference present in the data. Table 1 summarizes these 3 collections and indicates which measurement types were present in each collection. The measurement types include, but are not limited to, carrier-to-noise ratio, GNSS receiver on-board temperature, pseudorange (PSR), carrier phase (ADR), power spectral density samples, I/Q samples, and AGC settings.

Bobcat-1 had several tools dedicated to spectrum analysis. The spectrum collection mode collected PSD data and I/Q sample data, as well as observation and position data common to all of the Bobcat-1 collections. The PSD is composed of 204 bins each approximately 488 kHz in width, with a start frequency of 1531.5 MHz and stop frequency of 1630.6 MHz, Making for a bandwidth of approximately 100 MHz, centered on GPS L1 frequency. IQ samples are taken with respect to a frequency of 1562.5 MHz (GPS L1) at a sample rate of 25 Msps. A total of 20 ms of complex IQ samples is collected for each message. These I/Q samples will not be presented in this paper, but the AGC value derived from the I/Q samples will be.

Table 1: Type of measurements present in each data collection considered by this paper

ID	Type	C/N ₀	PSR	ADR	PSD	IQ	AGC
13	Spectrum	✓	✓			✓	✓
178	Spectrum	✓	✓			✓	✓
181	Time Offset	✓	✓	✓	✓		

1. Collection 13

Collection 13 the first spectrum type collection Bobcat-1 took on 21-Nov-2020 22:17:42. This collection had a runtime of 1h 30m 40s, almost completing one full orbit.

Figure 2 shows an example of a nominal PSD seen by Bobcat-1 throughout its operation, along with the location that the measurement was taken. Figure 3 shows an example of significant L1 interference, with the location it was seen at. It can be seen that there is approximately a 10 dBm increase from the noise floor.

Groundtracks of Bobcat-1 are overlaid with the maximum C/N₀ at the location for GPS L1 in figure 4. Locations where the

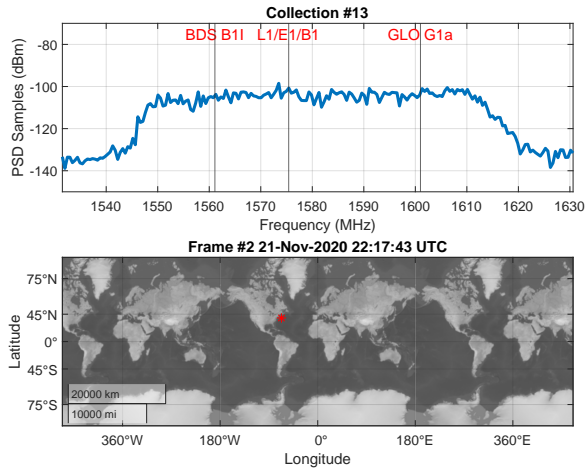


Figure 2: Groundtrack and nominal PSD for collection 13

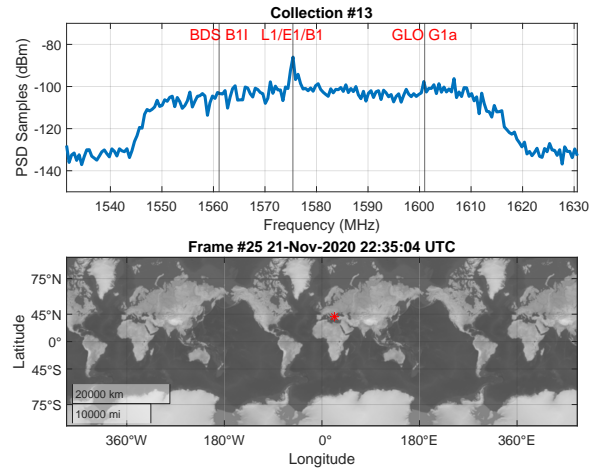


Figure 3: Groundtrack and interference affected PSD for collection 13

maximum C/N_0 was lower than 40 dB-Hz are highlighted in red. It should be known that this dataset has multiple time skips that represent periods when Bobcat-1 was not collecting any data. This is due to experiments with different collection modes.

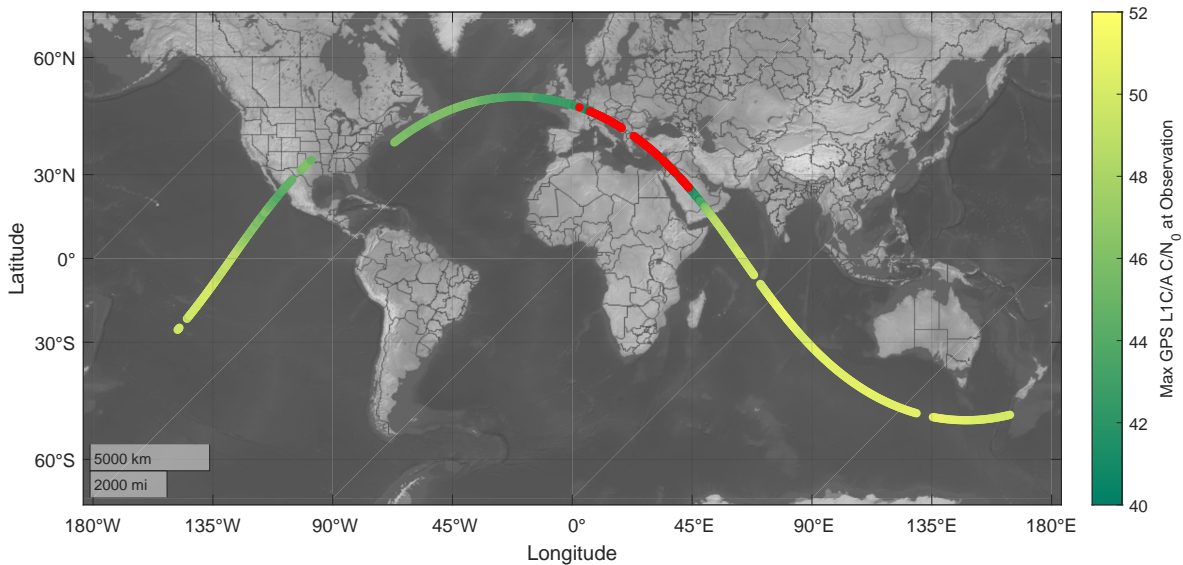


Figure 4: Groundtrack for collection 13; GPS L1

The following Figures 5 and 6 are similar to 4, except that they are plotted in time and represent GLONASS L1, Galileo E1, BDS B1C, and BDS(I), respectively. All the listed frequencies were captured by the PSD in figures 2 and 3. We can observe from figure 3, that at that time instant, Bobcat-1 should be experiencing significant interference at 1575 MHz. Indeed, at GNSS frequencies GPS L1, Galileo E1, and BDS B1C, the maximum C/N_0 has degraded. At frequencies further from 1575 MHz, such as BDS B1I, and GLONASS G1, we see much less of an effect on the maximum CNR.

The AGC for these samples is shown in figure 8 . It can be observed that a significant decrease in the AGC value over the same location that we saw a reduced C/N_0 .

Figure 9 shows the number of observations made by the Bobcat-1 receiver for several GNSS constellations. It can be observed that a large amount of observable are lost at 22:30 to 22:45 UTC, where Bobcat-1 experienced interference. There are two other points of interest at 22:18 and 23:30 UTC, where Bobcat-1 performs a reacquisition. Note that the large gap in observations from

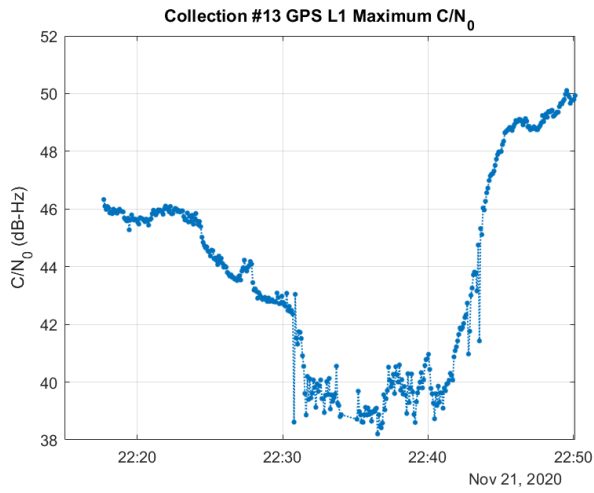


Figure 5: Maximum C/N_0 for GPS; GLONASS L1

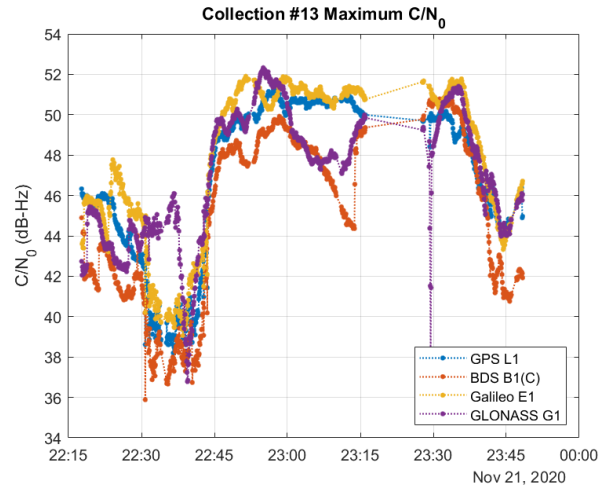


Figure 6: Maximum C/N_0 for GPS, BDS, Galileo, and GLONASS L1 frequencies.

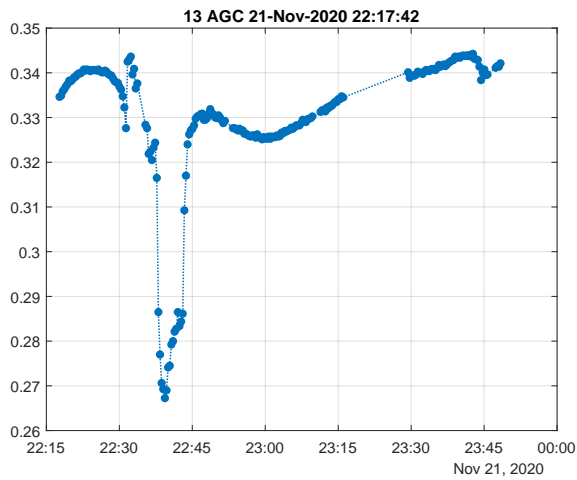


Figure 7: AGC for collection 13

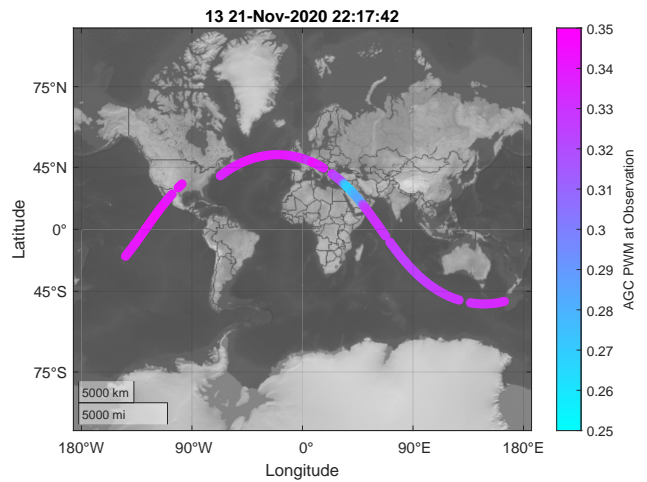


Figure 8: Groundtrack and AGC for collection 13

23:15 to 23:30 UTC was due to a programmed pause in the data collection. Figure 10 shows the number of GPS Observations by frequency. It can be seen that it follows a similar trend to figure 9.

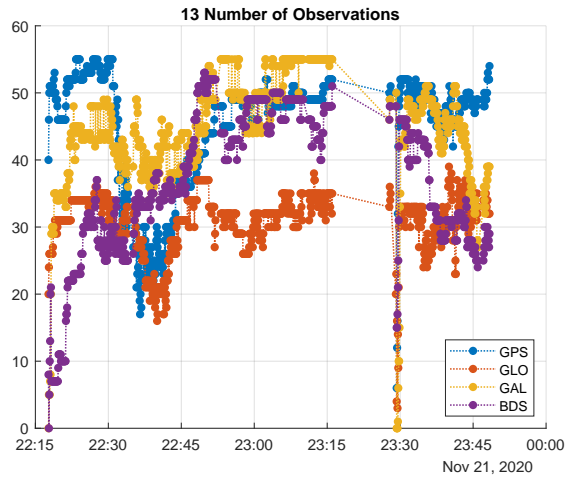


Figure 9: Number of GNSS observations for collection 13 by constellation

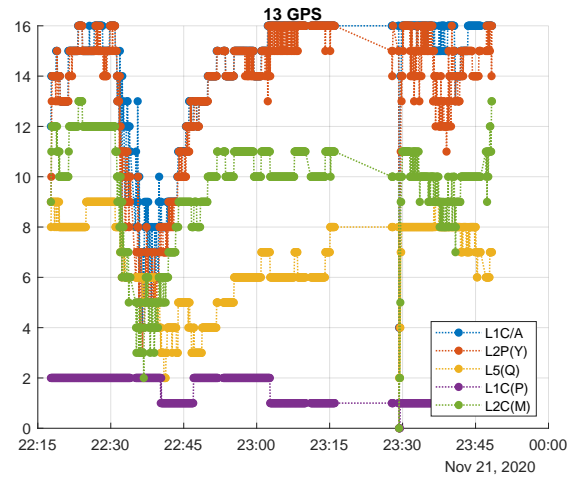


Figure 10: Number of GPS observations for collection 13 by frequency

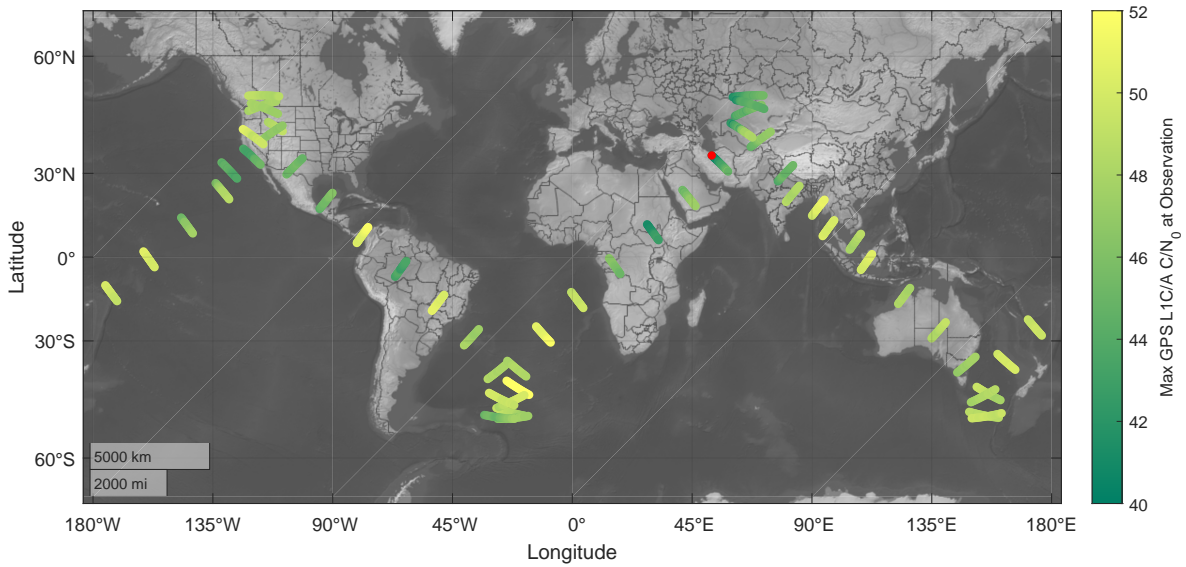


Figure 11: Groundtrack for collection 178; GPS L1;

2. Collection 178

Collection 178 started on 16-Dec-2021 19:36:07 and lasted 1d 3h 13m 15s, collecting 7.82 MB of information. Bobcat-1 made 17 complete orbits during this collection, encountering interference on multiple occasions. The spectrum collection mode for collection 178 records the same data as collection 13, but at different sample rates.

The collection 178 data collection mode took position, observation, and IQ sample measurements for 2 minutes every 30 minutes. As the orbit of Bobcat-1 is on average 01:30:00, this results in the groundtrack seen in figure 11. PSD was also taken every thirty minutes, but with only 5 samples taken over 30 seconds. Other parameters related to the PSD are unchanged from collection 13.

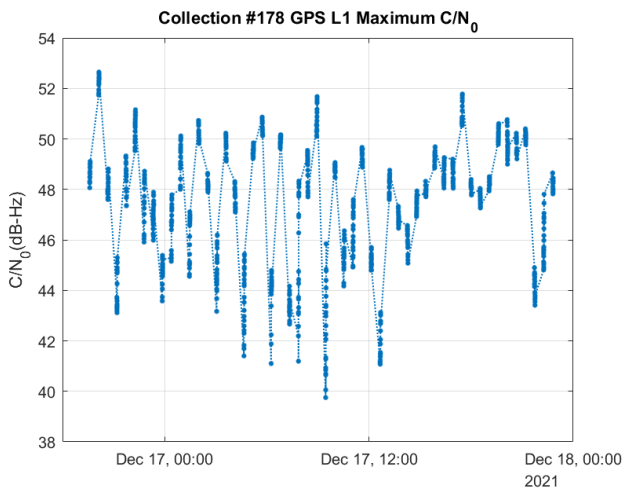


Figure 12: Maximum C/N_0 for GPS L1

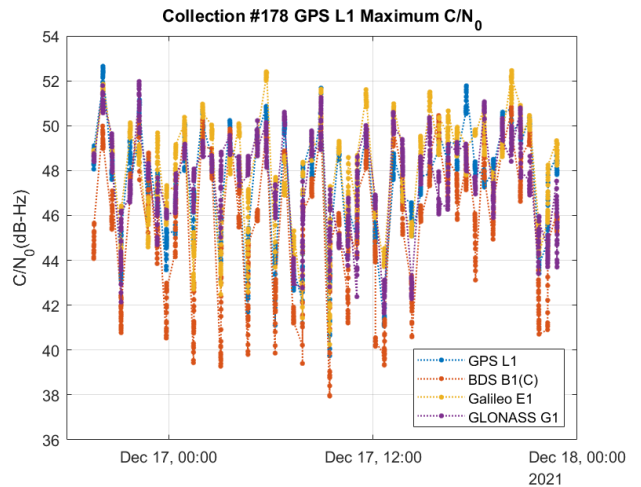


Figure 13: Maximum C/N_0 for GPS, BDS, Galileo, and GLONASS L1 frequencies.

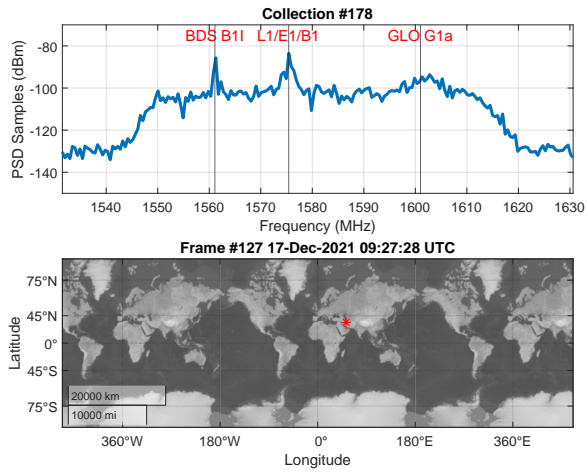


Figure 14: Groundtrack and PSD for collection 178 at a particular time. Interference can be seen in BDS B1 spectrums and GPS L1.

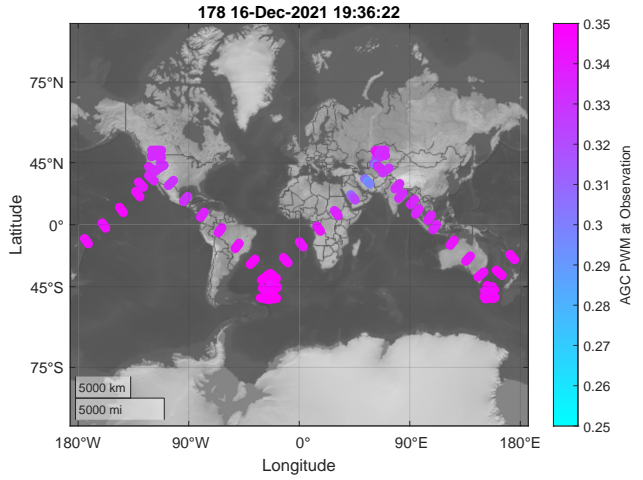


Figure 15: AGC groundtrack

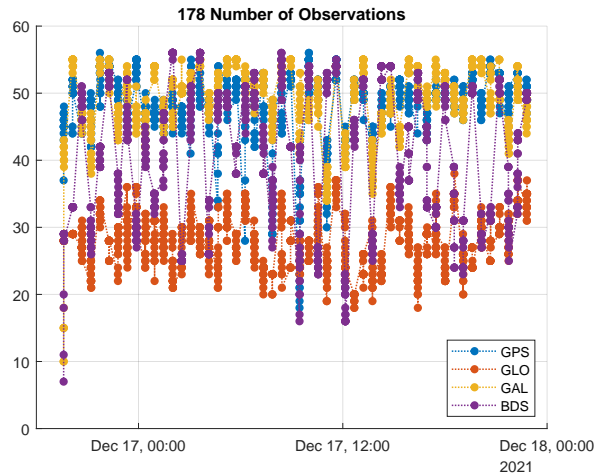


Figure 16: Number of Observations for 178

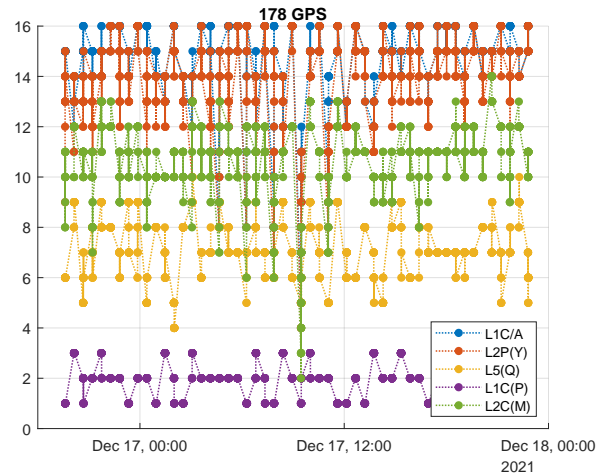


Figure 17: Number of observations over the collection period for GPS

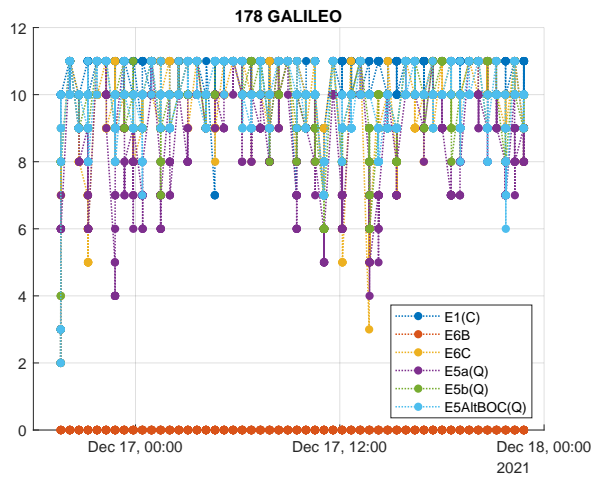


Figure 18: Number of observations over the collection period for Galileo

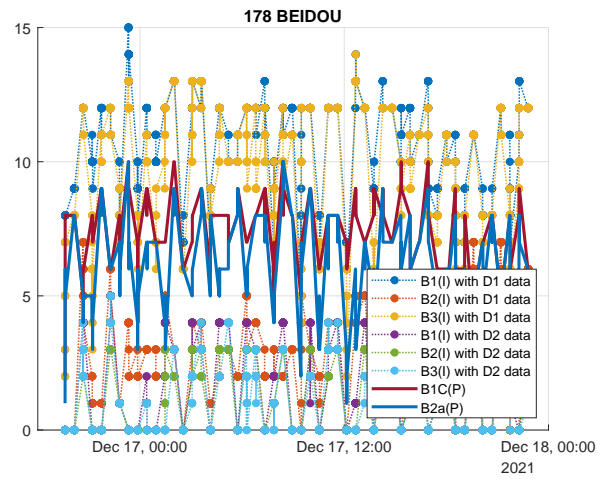


Figure 19: Number of observations over the collection period for Beidou

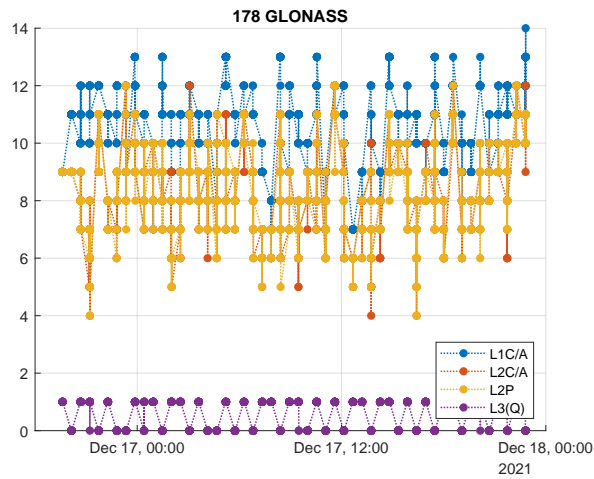


Figure 20: Number of observations over the collection period for GLONASS

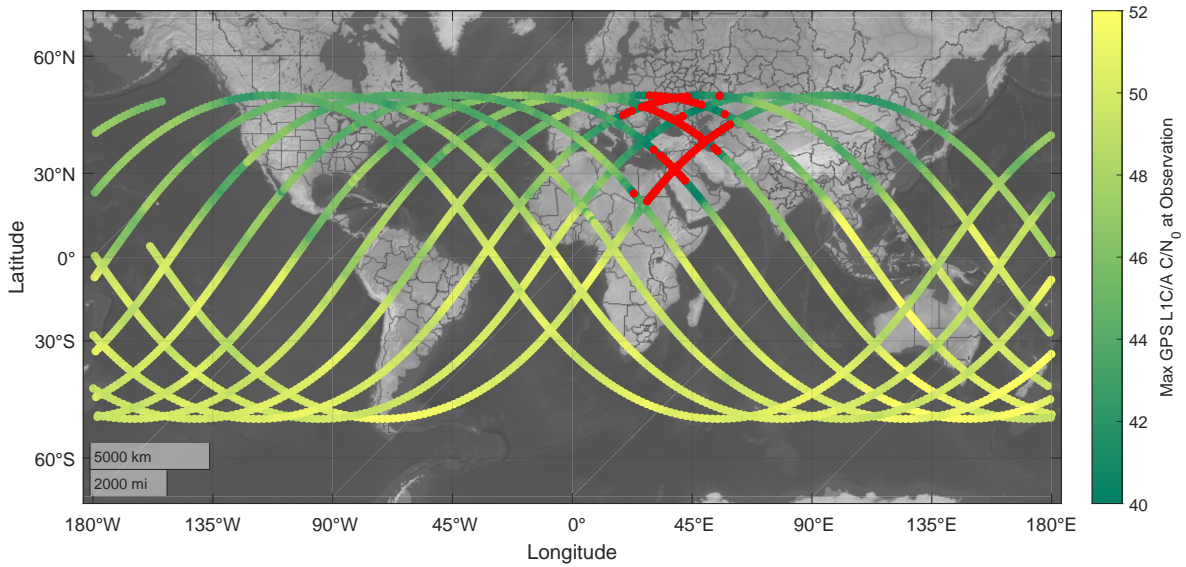


Figure 21: Groundtrack for collection 181; GPS L1;

3. Collection 181

Collection 181 started on 26-Dec-2021 21:45:02 UTC and lasted 16h 25m 20s, collecting 30.2 MB of information. Bobcat-1 made 16 complete orbits during this collection, encountering interference on multiple occasions. Collection 181 did not operate in the spectrum collection mode, but in the time offset mode. Bobcat-1 gathered observation data at a regular rate, making the continuous ground track seen in figure 21. As seen in collections 13 and 178, Bobcat-1 encounters significant interference in the PSD. Collection 181 does not have this metric, but it can be inferred from figure 21 that Bobcat-1 encounters significant interference over multiple passes.

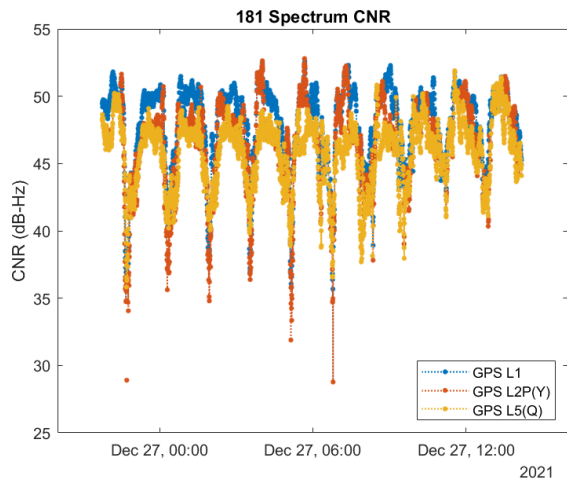


Figure 22: Maximum C/N_0 for GPS L1

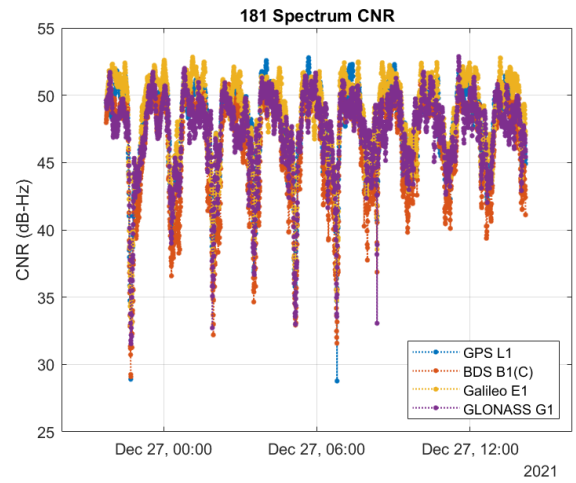


Figure 23: Maximum C/N_0 for GPS, BDS, Galileo, and GLONASS L1 frequencies.

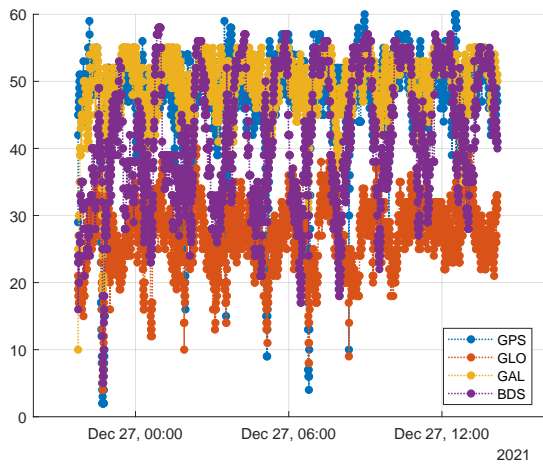


Figure 24: Number of Observations for 181

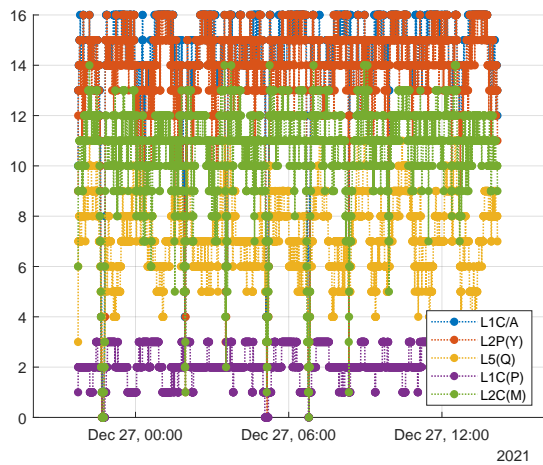


Figure 25: Number of observations over the collection period for GPS

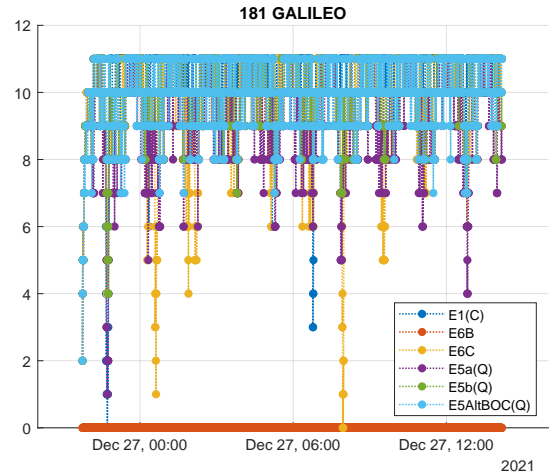


Figure 26: Number of observations over the collection period for Galileo

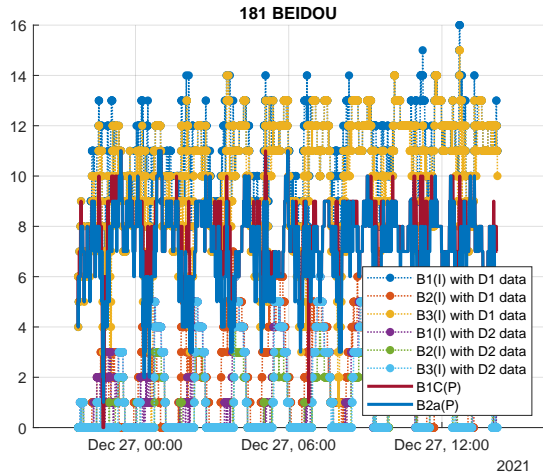


Figure 27: Number of observations over the collection period for Beidou

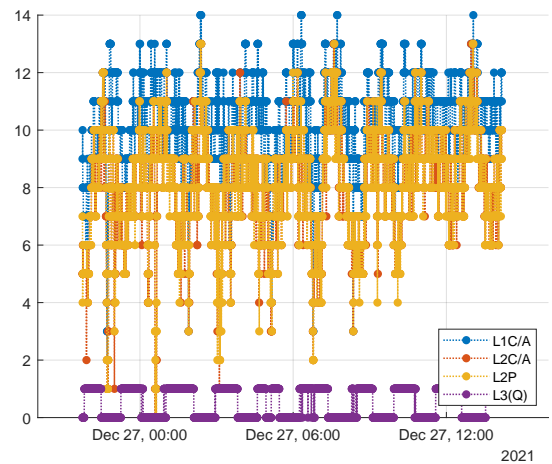


Figure 28: Number of observations over the collection period for GLONASS

III. CONCLUSIONS

While spectrum monitoring and interference were not Bobcat-1's main mission, we were still able to do an analysis on the affects of interference in LEO. Bobcat-1 had limited spectrum monitoring capabilities, but enough to deduce some of the characteristics of the interference. The interference seen throughout the lifespan of Bobcat-1 affected our ability to collect reliable data on GNSS, as seen briefly in other publications. Despite these interruptions, Bobcat-1's navigation capabilities were rarely impacted. The multi-GNSS multi-frequency capabilities of the Bobcat-1 receiver ensured Bobcat-1 kept a reliable position solution.

Further analysis will be performed to classify other interference events experienced during Bobcat-1 operations. For a more comprehensive analysis on the effects of interference on a CubeSat, it is recommended that the spectrum monitoring capabilities be improved in a future mission. Future work may include a theoretical C/N_0 at the reported position and be compared to the reported metric. Further modeling of the attitude of Bobcat-1 will be needed to bound the effects of the antenna on the evaluation of the interference.

IV. ACKNOWLEDGEMENTS

The authors would like to acknowledge NASA's Space Communications and Navigation Office (SCaN), NASA Glenn Research Center, NASA's CubeSat Launch Initiative (CSLI) and Ohio University for funding the Bobcat-1 CubeSat mission. Additionally, Kevin Croissant and Gregory Jenkins, previous student members of the Bobcat-1 team, and Dr. Frank van Graas, Ohio University Professor Emeritus and former faculty member of the Bobcat-1 team.

REFERENCES

- Allen, T. (2023, January). *Summary report of the 27th national Space-Based PNT Advisory Board meeting held 16-17 November 2022*. Space-Based Positioning, Navigation, and Timing (PNT) Advisory Board. Retrieved May 16, 2023, from <https://www.gps.gov/governance/advisory/recommendations/2023-01-PNTAB-27-chair-memo.pdf>
- Arnett, Z., McKnight, R., Ugazio, S., & van Graas, F. (2022). Receiver inter-constellation time offset at low Earth orbit: An experiment with Bobcat-1, the Ohio University CubeSat. *Proceedings of the 2022 International Technical Meeting of The Institute of Navigation*, 844–855. <https://doi.org/10.33012/2022.18176>
- Borio, D., O'Driscoll, C., & Fortuny, J. (2012). Gnss jammers: Effects and countermeasures. *2012 6th ESA Workshop on Satellite Navigation Technologies (Navitec 2012) & European Workshop on GNSS Signals and Signal Processing*, 1–7. <https://doi.org/10.1109/NAVITEC.2012.6423048>
- CaJacob, D., McCarthy, N., O'Shea, T., & McGwier, R. (2016). Geolocation of RF emitters with a formation-flying cluster of three microsatellites [SSC16-VI-5]. *Proceedings of the AIAA/USU Conference on Small Satellites*. <https://digitalcommons.usu.edu/smallsat/2016/TS6NextOnPad/5/>
- Clements, Z., Ellis, P., Psiaki, M., & Humphreys, T. E. (2022). Geolocation of terrestrial GNSS spoofing signals from low Earth orbit. *Proceedings of the 35th International Technical Meeting of the Satellite Division of The Institute of Navigation (ION GNSS+ 2022)*, 3418–3431. <https://doi.org/10.33012/2022.18444>
- Clements, Z., Humphreys, T. E., & Ellis, P. (2023). Dual-satellite geolocation of terrestrial gnss jammers from low earth orbit. *2023 IEEE/ION Position, Location and Navigation Symposium (PLANS)*, 458–469. <https://doi.org/10.1109/PLANS53410.2023.10140058>
- Dacus, M., Liu, Z., Lo, S., & Walter, T. (2022). Improved RFI localization through aircraft position estimation during losses in ADS-B reception. *Proceedings of the 35th International Technical Meeting of the Satellite Division of The Institute of Navigation (ION GNSS+ 2022)*, 947–957. <https://doi.org/10.33012/2022.18529>
- Ellis, P., Irisov, V., Pojani, G., Binda, S., Khan, H., Cappaert, J., Yuasa, T., & Nogués-Correig, O. (2022). GNSS interference monitoring from LEO using the Spire constellation. *Proceedings of the 4S Symposium: Small Satellites Systems and Services*.
- Falletti, E., Falco, G., Nguyen, V. H., & Nicola, M. (2021). Performance analysis of the dispersion of double differences algorithm to detect single-source gnss spoofing. *IEEE Transactions on Aerospace and Electronic Systems*, 57(5), 2674–2688. <https://doi.org/10.1109/TAES.2021.3061822>
- GNSS interference report: Finland*. (2022, September). Aurora Insight. Retrieved June 9, 2023, from <https://aurorainsight.com/resource/finland/>
- Jada, S., Bowman, J., Psiaki, M., Fan, C., & Joerger, M. (2022). Time-frequency analysis of GNSS jamming events detected on U.S. highways. *Proceedings of the 35th International Technical Meeting of the Satellite Division of The Institute of Navigation (ION GNSS+ 2022)*, 933–946. <https://doi.org/10.33012/2022.18528>
- LaChapelle, D. M., Narula, L., & Humphreys, T. E. (2021). Orbital war driving: Assessing transient GPS interference from LEO. *Proceedings of the 34th International Technical Meeting of the Satellite Division of The Institute of Navigation (ION GNSS+ 2021)*, 3556–3568. <https://doi.org/10.33012/2021.17986>
- Liu, Z., Lo, S., Walter, T., & Blanch, J. (2022). Real-time detection and localization of GNSS interference source. *Proceedings of the 35th International Technical Meeting of the Satellite Division of The Institute of Navigation (ION GNSS+ 2022)*, 3731–3742. <https://doi.org/10.33012/2022.18562>
- Miguel, N. R. S., Chen, Y.-H., Lo, S., Walter, T., & Akos, D. (2022). Stress testing of a low-cost gnss rfi monitor. *Proceedings of the 35th International Technical Meeting of the Satellite Division of The Institute of Navigation (ION GNSS+ 2022)*, 3463–3478. <https://doi.org/10.33012/2022.18444>

- Miguel, N. R. S., Chen, Y.-H., Lo, S., Walter, T., & Akos, D. (2023). Calibration of rfi detection levels in a low-cost gnss monitor. *2023 IEEE/ION Position, Location and Navigation Symposium (PLANS)*, 520–535. <https://doi.org/10.1109/PLANS53410.2023.10140085>
- Murrian, M. J., Narula, L., Iannucci, P. A., Budzien, S., O'Hanlon, B. W., Psiaki, M. L., & Humphreys, T. E. (2021). First results from three years of GNSS interference monitoring from low Earth orbit. *NAVIGATION: Journal of the Institute of Navigation*, 68(4), 673–685. <https://doi.org/10.1002/navi.449>
- Nasser, H., Berz, G., Gómez, M., de la Fuente, A., Fidalgo, J., Li, W., Pattinson, M., Truffer, P., & Troller, M. (2022). GNSS interference detection and geolocalization for aviation applications. *Proceedings of the 35th International Technical Meeting of the Satellite Division of The Institute of Navigation (ION GNSS+ 2022)*, 192–216. <https://doi.org/10.33012/2022.18358>
- OEM7 commands and logs reference manual*. (2023, May). Version 23. NovAtel. Retrieved June 12, 2023, from https://docs.novatel.com/OEM7/Content/PDFs/OEM7_Commands_Logs_Manual.pdf
- Spens, N., Lee, D.-K., Nedelkov, F., & Akos, D. (2022). Detecting GNSS jamming and spoofing on Android devices. *NAVIGATION: Journal of the Institute of Navigation*, 69(3). <https://doi.org/10.33012/navi.537>
- Teunissen, P. J., & Montenbruck, O. (2017). *Springer handbook of global navigation satellite systems* (Vol. 10). Springer.
- Ward, P. W., Betz, J. W., & Hegarty, C. (2017). GNSS disruptions. In E. D. Kaplan & C. J. Hegarty (Eds.), *Understanding GPS/GNSS: Principles and applications* (3rd ed., pp. 549–618). Artech House.